Label-free flow cytometry using multiplex coherent anti-Stokes Raman scattering (MCARS) for the analysis of biological specimens

Charles H. Camp, Jr.,[1] Siva Yegnanarayanan,[1,2] Ali A. Eftekhar,[1] and Ali Adibi[1,*]

[1]*School of Electrical and Computer Engineering, Georgia Institute of Technology, 777 Atlantic Drive, Atlanta, Georgia 30332, USA*

[2]*Currently with Lincoln Laboratory, Massachusetts Institute of Technology, 244 Wood Street, Lexington, Massachusetts 02420, USA*

**Corresponding author: ali.adibi@ece.gatech.edu*

Received April 5, 2011; revised May 11, 2011; accepted May 18, 2011;
posted May 19, 2011 (Doc. ID 144599); published June 14, 2011

We present the first demonstration, to our knowledge, of a label-free flow cytometer for the analysis of biological specimens using multiplex coherent anti-Stokes Raman scattering (MCARS) and elastic scatter measurements. The MCARS system probes the Raman vibrational energy levels and the elastic scatter provides morphological information. We demonstrate these capabilities by probing a culture of *Saccharomyces cerevisiae* at 100 spectra/s and constructing a background-free Raman reconstruction using a Kramers–Kronig relation. A theoretical analysis shows that this system could operate at speeds of 10 kHz with appropriate hardware; thus facilitating integration into commercial flow cytometers or use as a high-speed, stand-alone device.

OCIS codes: 190.4380, 190.7110, 300.6230.

Flow cytometry is an advanced, multivariate tool that incorporates optics and electronics to measure an ever-growing variety of phenotypes [1]. Flowing samples are interrogated by one or more lasers, and the elastically scattered photons are measured to ascertain morphological information. Acquiring molecular information, however, requires the addition of fluorescent labels. Although a powerful tool, these labels present challenges such as large emission spectra and cytotoxicity, which can alter cellular chemistries and perturb experimental outcomes [1,2]. Additionally, the process of conjugating fluorophores and labeling cells can be time consuming, thus reducing clinical turnaround times and affecting time-sensitive samples. Label-free technologies, such as Raman spectroscopy and coherent anti-Stokes Raman scattering (CARS), which have seen tremendous growth in the microscopy community, offer attractive possibilities for label-free flow cytometry.

Raman scattering spectroscopy is a powerful tool for probing intrinsic vibrational energy levels within sample molecules. As a spontaneous optical process, however, this technique requires long integration times that make its use in high-speed flow cytometry unfeasible [3]. To combat these shortcomings, a family of coherent Raman techniques based on CARS has been developed that under many biologically relevant conditions operates with efficiency that is orders of magnitude higher than spontaneous Raman spectroscopy, facilitating vibrationally sensitive imaging—even at video rates [4–6]. Although CARS has been applied to flow cytometry [7], the generation of a nonresonant background (NRB) produces signals for all samples regardless of whether a Raman transition is being probed. Practical application of CARS to flow cytometry requires probing multiple Raman vibrational energy levels to obtain a more complete spectral picture and to disambiguate resonant and nonresonant signal contributions—a task possible through broadband implementations of CARS such as multiplex CARS (MCARS) [8] and broadband CARS (BCARS) [9].

Previously, we reported on the first construction of a label-free flow cytometer using MCARS and applied it to differentiating polymer beads of similar morphologies [10]. To extract higher levels of information about sample composition, however, requires the additional measurement of elastically scattered photons [1]. Although traditional flow cytometers employ a large area of light to interrogate passing samples, probing cells with focused beams (i.e., "slit-scanning") provides improved sizing capabilities and morphological information [1]. We anticipate that this unique combination of focused beam elastic scatter measurement and MCARS will provide information that may not be available using conventional flow cytometry. Figure 1 is a schematic of our MCARS flow cytometer. This system uses a femtosecond source at 806 nm to pump the CARS process (~60 mW at sample, ~86 MHz repetition rate, bandpass filtered to <6 nm FWHM) and to seed a microstructured fiber that generates a broadband Stokes source (~10 mW at sample). The excitation sources are coupled into an inverted microscope and focused onto a glass flow cell ($100 \times 300\,\mu$m flow channel) with a 100× objective (NA = 1.25). The scattered photons are collected in the forward direction with a 10× long-working distance objective (NA = 0.25)

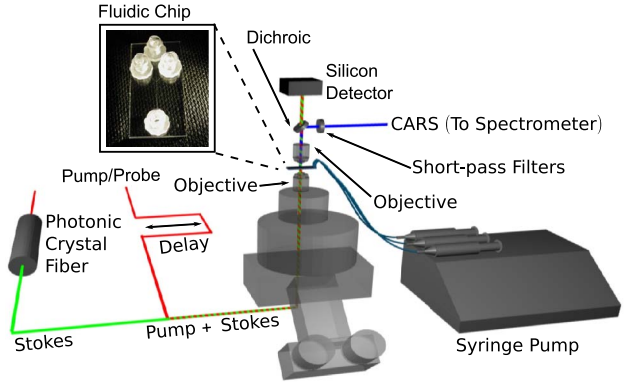

Fig. 1. (Color online) Schematic of the label-free MCARS flow cytometer.

and filtered by a long-pass dichroic beam splitter. The longer wavelengths are measured by an amplified silicon detector to gauge the elastically forward-scattered photons (FSC). The voltage of this detector is recorded at up to 1.25 MHz by a data-acquisition board. The anti-Stokes photons are coupled into a CCD spectrometer, which contains a two-dimensional CCD chip (1024 × 256 pixels) that is operated with full vertical binning and 8-pixel horizontal (spectral) binning to capture each ~84 nm(1756 cm^{-1}) bandwidth spectrum. Data recording and gating are performed in LabView, and final processing and analysis are performed in MATLAB.

To illustrate the capabilities of the label-free flow cytometer, we analyzed a culture of *S. cerevisiae*, a yeast often used to model higher eukaryotic organisms such as humans. The MCARS spectra of the flowing cells (~2×10^8/mL, velocity ~4.3 mm/s) were recorded at 100 Hz and the FSC recorded at 10 kHz. The gating was performed in software and triggered from changes to the FSC. Figure 2(a) is a density scatter plot of the maximum versus the minimum FSC for 7685 cells. The baseline FSC (i.e., no particles are present) is ~6 V. One can clearly see two subpopulations: one with a substantial voltage above the baseline, and the other, predominantly below. Figure 2(b) represents two individual elastic scatter measurements taken from each region that typify the aforementioned effect. The exact shape of the FSC waveform is dependent on the refractive and diffractive effects due to the cell size, shape, and internal complexity and structure. Additionally, the high NA excitation objective creates a large cone of light that probes the cell over a large volume; thus, the transit time recorded in the elastic scatter measurement may be elongated from the actual transit time through the focal volume (~2–4 ms). The subpopulation with the larger maximum FSC is likely to contain cells with internal scatterers (such as lipid vacuoles) that provide a mechanism for constructive interference between the incident beam and the scattered photons, whereas the lower maximum FSC population contains fewer scatterers; thus, the incident beam is only slightly refracted due to the near index

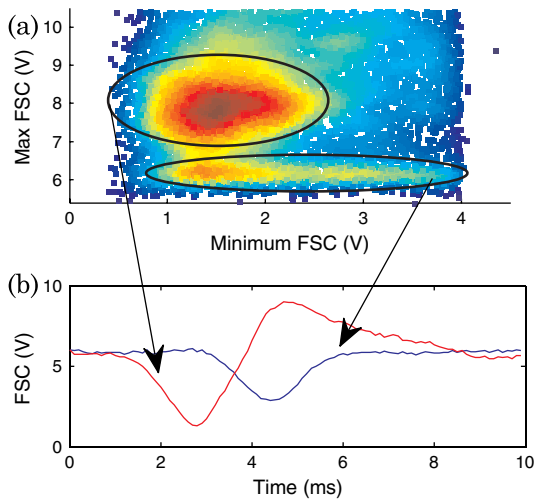

Fig. 2. (Color online) (a) Density scatter plot of maximum FSC voltage versus minimum FSC voltage for *S. cerevisiae*. (b) Two representative time traces of FSC from within the two subpopulations in (a).

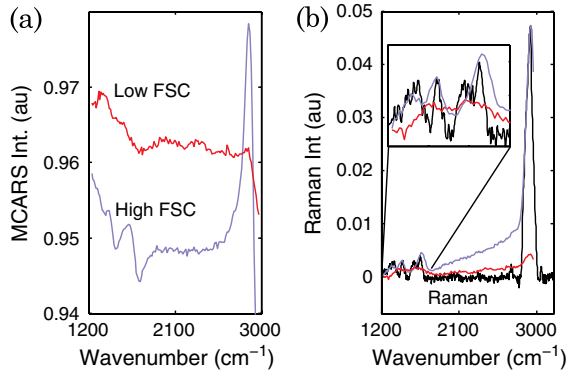

Fig. 3. (Color online) (a) Mean MCARS spectrum of the subpopulations of yeast in Fig. 2(a) with high- (blue) and low- (red) maximum FSC. Corresponding reconstructed Raman spectrum compared to the spontaneous Raman spectrum of a lipid-rich yeast (black).

matching between the cytoplasm and the aqueous sample flow [11]. Figure 3(a) shows the mean MCARS spectra (normalized to the spectrum of water) for the two subpopulations described in Fig. 2(a). One can see that the high-maximum FSC population exhibits strong spectral peaks at 1411, 1624, and 2867 cm^{-1}. Because of the coherent mixing between the NRB and the resonant CARS signal, MCARS spectral peaks are typically distorted from their spontaneous Raman counterparts. To counteract these effects, we applied a Kramers–Kronig transform technique for spectral reconstruction, using the raw MCARS spectrum of the yeast as the signal and the spectrum of the aqueous background as the estimated NRB [12]. Figure 3(b) shows the mean reconstructed spectra for the two yeast subpopulations and a Raman spectrum collected from a lipid-rich yeast collected on a commercial micro-Raman system. For the high-maximum FSC subpopulation, four peaks are resolved at 1318, 1442, 1662, and 2935 cm^{-1} that correspond closely with those found in the spontaneous Raman spectrum at 1328 cm^{-1}, 1442 cm^{-1} (CH_2-deformation), 1652 cm^{-1} (amide I), and 2930 cm^{-1} (CH-stretch). The low-FSC subpopulation resolves only a single clear peak around 2935 cm^{-1} and two broad, weak peaks around 1582 cm^{-1} and 1430 cm^{-1}. Based on this analysis, we see that, indeed, the high-FSC population contains more prominent lipid-rich internal scatterers than the low-FSC population. In this yeast culture, ~71% of the cells measured exhibited a prominent CH-stretch peak associated with the lipid-rich organelles within the cells [5]. This agrees closely with the measurement performed with a commercial flow cytometer using Nile Red lipophilic stain (~72%).

The presented analysis demonstrates the ability of MCARS flow cytometry to measure the MCARS spectrum of flowing biological specimens with a high signal-to-noise ratio (SNR) (>10 dB) and to collect elastic scatter information, which can be further analyzed to reveal morphological features. The high SNR and commercial availability of high-speed CCD spectrometers indicate that this system can act at higher speeds with appropriate hardware and triggering. Currently, the system is limited to fixed 10 ms acquisition times; thus, each MCARS spectrum is a linear combination of anti-Stokes photons from

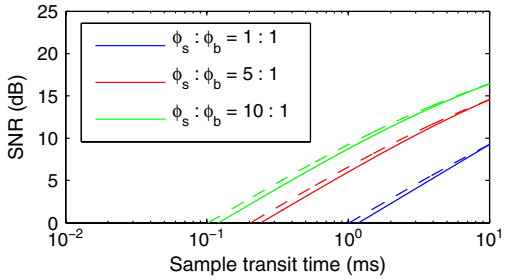

Fig. 4. (Color online) SNR versus cell transit time under different ratios of the photon flux of anti-Stokes photons to background photons from the water. Solid curves are calculated using Eq. (1) for the system operating at 100 Hz; dashed curves are for ideal gated CCD recording.

the sample and from the aqueous background. The minimum transit time is determined by the relative emission intensities of the sample and the aqueous background, as well as by the detector and total shot noise. The SNR versus the transit time is modeled as

$$\mathrm{SNR} = \phi_s \eta M t_s \times \{[\phi_s t_s + \phi_b (T - t_s)]\eta M + \mathrm{DMT} + N_r^2\}^{-1/2}, \quad (1)$$

where t_s is the sample transit time; T, the integration time; ϕ_s and ϕ_b, the photon flux of the CARS process and the aqueous background, respectively; and η, M, D, and N_r, the CCD quantum efficiency, pixel binning, dark current, and read noise, respectively. Figure 4 (solid curves) shows the SNR versus transit time for various signal-to-background ratios (SBR). The background photon flux was measured under typical conditions (~24/ pixel/s); manufacturer specifications were used for η(~50%), $D(0.001\,\mathrm{e}^{-1}/\mathrm{pixel/s})$, and $N_r(24\,\mathrm{e}^{-1})$ rms. A sample's SBR is determined by a number of factors such as excitation pulse lengths and the molecular scatterer concentration. For the culture presented in Fig. 3, the calculated SBRs ranged from 2–12, with the average CH-stretch SBR being ~9.1. With the current system's fixed integration times, the system is limited to sample transit times of ~0.12–1.2 ms. With future hardware improvements facilitating triggered acquisition during which the sample is within the focal volume and high-speed data transfer rates (dashed curves in Fig. 4), the minimum transit time for a sample with a SBR of ~9.1 would decrease from 0.12 ms to 0.1 ms and would allow an acquisition speed of ~10 kHz that would facilitate integration with commercial flow cytometers (~1–20 kHz acquisition).

Label-free flow cytometry using MCARS is a valuable tool for probing a broad bandwidth of the intrinsic Raman energy levels at high-speed. We have demonstrated the applicability of this technique to biological specimens by probing a culture of yeast at 100 Hz. This acquisition rate represents the fastest evaluation of Raman spectra in flow cytometry to date; although, this technique is theoretically capable of 10 kHz acquisition with appropriate and feasible hardware improvements. Additional improvements to excitation sources and detectors further opens this technique's integration with traditional flow cytometry or as a stand-alone device.

The authors wish to thank Dr. Marcus Cicerone at the National Institute of Standards and Technology (NIST) for his assistance with the Kramers–Kronig reconstruction software. Additionally, the authors wish to thank the reviewers for their helpful advice and discussion.

References

1. H. M. Shapiro, *Practical Flow Cytometry*, 4th ed. (Wiley Liss, 2003).
2. N. Baumgarth and M. Roederer, J. Immunol. Methods **243**, 77 (2000).
3. A. Y. Lau, L. P. Leeb, and J. W. Chan, Lab Chip **8**, 1116 (2008).
4. C. L. Evans and X. S. Xie, Ann. Rev. Anal. Chem. **1**, 883 (2008).
5. C. Brackmann, J. Norbeck, M. Åkeson, D. Bosch, C. Larsson, L. Gustafsson, and A. Enejder, J. Raman Spectrosc. **40**, 748 (2009).
6. H. W. Wang, N. Bao, T. T. Le, C. Lu, and J. X. Cheng, Opt. Express **16**, 5782 (2008).
7. M. Müller and J. M. Schins, J. Phys. Chem. B **106**, 3715 (2002).
8. S. H. Parekh, Y. J. Lee, K. A. Aamer, and M. T. Cicerone, Biophys. J. **99**, 2695 (2010).
9. C. H. Camp, S. Yegnanarayanan, A. A. Eftekhar, and A. Adibi, Opt. Express **17**, 22879 (2009).
10. A. L. Koch, B. R. Robertson, and D. K. Button, Methods Microbiol. **27**, 49 (1996).
11. Y. Liu, Y. J. Lee, and M. T. Cicerone, Opt. Lett. **34**, 1363 (2009).
12. M. Cui, B. R. Bachler, and J. P. Ogilvie, Opt. Lett. **34**, 773 (2009).